Theory of interface-roughness scattering in resonant tunneling

Peter Johansson
NORDITA, Blegdamsvej 17, DK-2100 Copenhagen, Denmark
(Received 22 February 1993)

We have calculated the effects of interface-roughness scattering on resonant tunneling through a GaAs-$Al_xGa_{1-x}As$ double-barrier structure. In our calculation we treat the double-barrier potential exactly. The interface-roughness scattering is dealt with nonperturbatively by means of the self-consistent Born approximation, which preserves unitarity. In the presence of scattering, the peak current is reduced by ~10%, but not more, even though a tunneling electron may be scattered many times while inside the quantum well. The valley current, on the other hand, is increased by several orders of magnitude due to the scattering if the barriers are thick enough. For thin barriers, the calculated peak-to-valley (P/V) ratios increase exponentially with the barrier thickness. At a barrier thickness of ≈100 Å the P/V ratio crosses over to a much slower increase, and eventually reaches a maximum, after that the P/V ratio decreases somewhat. This qualitative behavior is in good agreement with recent experimental results. A surprising result of this work is that nonperturbative and perturbative calculations give practically identical results for the valley current for realistic parameter values for the interface roughness.

I. INTRODUCTION

Molecular-beam epitaxy (MBE) has made it possible to build artificial structures and materials such as quantum wells and superlattices. The resonant tunneling double-barrier structure (DBS) is one of the systems that has been most extensively studied in this context. By growing alternating layers of two semiconductors, typically GaAs and $Al_xGa_{1-x}As$, with different band gaps, on top of each other one can create a structure in which the effective potential felt by an electron is close to an ideal double-barrier model potential. Thus, as a first approximation the tunneling transmission probability and subsequently the tunnel current can be calculated by assuming that the tunneling is fully coherent. One applies wave mechanics to a square-barrier model of the semiconductor DBS. In such a calculation it is assumed that the momentum of a tunneling electron parallel to the barriers is conserved.[1]

This type of theory does indeed reproduce the most conspicuous feature of the current-voltage characteristics of a DBS, namely the negative differential resistance behavior. As the bias voltage across the structure is increased, the tunnel current initially increases and reaches a peak value. If the bias voltage is further increased, the resonant state in the quantum well, through which most of the tunnel current passes, is pulled below the bottom of the conduction band of the doped emitter contact. At this point the tunnel current drops substantially and the so-called valley current is obtained. Finally, for even higher voltages the current increases again, either due to resonant tunneling through resonant levels of higher energy or because the downstream barrier begins to collapse so that field emission sets in.

The results of the simple theory described above are, however, not in complete quantitative agreement with experiment. Most importantly, in many cases the calculated values of the valley current are too small. This is not surprising since a number of scattering processes that are not present in a double-barrier model potential occur in the DBS. The electrons can, for example, interact with the phonon modes of the DBS materials, and this leads to important modifications of the current-voltage characteristics.[2] In this work we will treat another important process, namely the scattering of the tunneling electrons off the rough interfaces between the barriers and the quantum well. The structure grown by MBE is not identical to an ideal DBS with perfectly flat interfaces between the different materials. The sharpness of an interface can only be controlled to within two to three atomic layers, so there will inevitably be steps and islands etc., on the interfaces.[3,4] This gives rise to a scattering potential. The elastic interface-roughness scattering assists tunneling by transferring energy, from an electron's motion perpendicular to the barriers, to the parallel motion, or vice versa. In this way an electron that enters the quantum well with a perpendicular-motion energy that is off resonance can be brought into resonance.

Longitudinal-optical (LO) phonons and interface roughness are generally considered to be the two most important causes of scattering in a DBS. Which one is more important depends on the geometric parameters and barrier composition of the DBS and the temperature. In this study we will focus on DBS's with thick and low barriers; interface roughness is expected to cause the most important scattering processes in these structures. Guéret *et al.*[5,6] have carried out a systematic study of how the barrier thickness affects the current-voltage characteristics. They used DBS's with well width L =70 Å, barrier thicknesses d varying between 75 and 310 Å, and barrier height V_b =120 meV. The experiments were performed at a temperature of 4.2 K. The low barrier height has the advantage that band bending only gives small effects. The low temperature prevents LO-phonon absorption processes from taking place; there are no thermally excited LO phonons. Phonon emission does not affect the

0163-1829/93/48(12)/8938(10)/$06.00

valley current too much. Resonant tunneling through the LO-phonon emission sideband of the DBS mainly plays a role at bias voltages that are so large that the DBS has already entered the field emission regime. The measured peak current agreed well with what is found from a calculation within the coherent picture. The valley current was, on the other hand, many orders of magnitude larger in the experiment than in the theoretical calculation if only the barriers were thick enough. The experimental peak-to-valley (P/V) ratio reached a constant value of ≈ 20 for barriers thicker than 100–150 Å. In their papers Guéret *et al.* suggest that the low P/V ratios are primarily the result of interface-roughness scattering.

On the theory side, a large number of papers treating phonon[7–14] and interface-roughness[15–23] scattering and related effects[24,25] have been published. Common to almost all of the theories of interface-roughness scattering is a perturbative treatment of the roughness. In this paper we will calculate the effects of interface roughness on resonant tunneling nonperturbatively. In a DBS with thick barriers a tunneling electron is trapped inside the quantum well for a long time. For a DBS with 200-Å-thick barriers, for example, the intrinsic lifetime of an electron inside the quantum well, estimated from the width of the transmission resonance, is of the order of 5 ns. The time between different scattering events can be much shorter. If there is one resonant state in the quantum well that is energetically accessible for the tunneling electron, an estimate of the scattering lifetime can be found from the golden rule, assuming that the scattering potential is equal to the change of the resonant level energy when the width of the quantum well is changed. We get

$$\frac{1}{\tau_{sc}} = \frac{2\pi}{\hbar} n_i A_i^2 \, 4\varepsilon_0^2 \left(\frac{\delta L}{L}\right)^2 \frac{m^*}{2\pi\hbar^2}, \tag{1}$$

where n_i is the number of roughness islands per unit area, A_i is their average area, ε_0 is the resonant energy and δL is the change of the quantum well width L due to a roughness island. The last factor comes from the sum over final states, and m^* is the electron effective mass. Note that $\varepsilon_0 \sim 1/L^2$ so that $1/\tau_{sc} \sim 1/L^6$. With typical parameter values ($n_i = 10^{-5}$ Å^{-2}, $A_i = 4\times10^4$ Å^2, $\varepsilon_0 = 40$ meV, $m^* = 0.067 m_0$, and $\delta L/L = 0.05$), we get $\tau_{sc} \approx 0.2$ ps. Thus the intrinsic lifetime is usually much longer than the scattering lifetime and an electron will typically be scattered many times while inside the quantum well. The interface-roughness scattering must be treated to infinite order in order to obtain a complete description of the resonant tunneling in such a case.

At the same time as we treat the scattering to infinite order we will also average over different roughness configurations. This introduces a dephasing mechanism into the calculation. It is not immediately clear that such a procedure is valid since we are dealing with an elastic-scattering process in a mesoscopic device. However, we argue that configuration averaging should work when calculating an integrated quantity such as the tunnel current. Numerical studies by Fertig, He, and Das Sarma[19] indicate that the configuration-averaged transmission probability gives a smoothened average of the rapidly varying, exact transmission probability resulting from a given roughness realization. In this context we should mention the work by Büttiker[26] in which he developed a description of incoherent resonant tunneling by means of connecting the quantum well to a (hypothetical) dephasing lead. Hershfield[27] has shown that treating impurity scattering to infinite order while at the same time averaging over configurations is equivalent to the application of dephasing leads.

In a recent publication[28] we reported on a nonperturbative calculation of the effects of interface-roughness scattering on resonant tunneling. In what follows we will improve on the earlier calculation. The double-barrier structure in Ref. 28 was treated by a transfer Hamiltonian. This means that it is not possible to get a very accurate description of the tunnel current at large bias voltages. In this work we treat the double-barrier potential exactly. Consequently the present formalism is able to describe correctly the onset of field emission at large bias voltage. The second major improvement is that we will take into account the finite lateral extension of the interface-roughness islands. In our earlier calculation each roughness island was modeled by a δ-function potential. This leads to an overestimation of the roughness-assisted contribution to the tunnel current since there is no upper limit on the change of an electron's parallel momentum in each scattering event. Here we instead model each island with a Gaussian potential with an effective cutoff at a momentum transfer of the order of $\hbar/\rho_0$, where ρ_0 is the typical radius of an interface-roughness island.

The results of our calculation are in good qualitative agreement with the experiment of Guéret *et al.*[6] We find that the peak current is not changed much when the effects of scattering are included in the calculation, but the valley current increases by several orders of magnitude if the barriers are thick. Our calculated P/V ratio grows rapidly with increasing barrier thickness d up to $d \approx 100$ Å. After that the increase is slower and finally for barriers thicker than $d \approx 200$ Å the P/V ratio even decreases slightly. We have also compared the results of the nonperturbative calculation with what one gets when treating the interface roughness to lowest order in perturbation theory. The surprising result is that the valley currents obtained from the two different calculations are basically identical, despite the principally very different descriptions of the physics.

The rest of the paper is organized in the following way: In Sec. II we develop the formalism necessary in order to treat the interface-roughness scattering to infinite order. In Sec. III we present and discuss the results of our calculations. Section IV, finally, gives a summary.

II. THEORY

A. Transmission probability and the tunnel current

In this section we will calculate the tunnel current density through the double-barrier structure schematically illustrated in Fig. 1. We will use scattering-theoretic methods in the calculation. We do not take into account

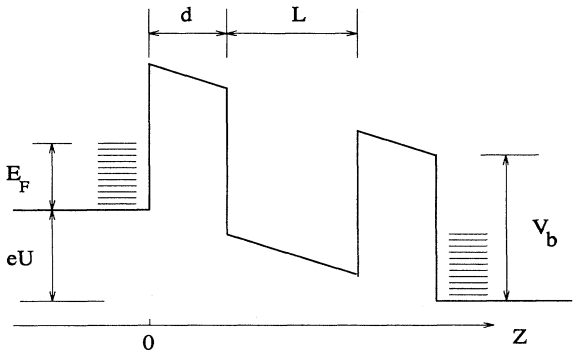

FIG. 1. Schematic illustration of the double-barrier structure considered in this work.

any electron-electron interaction. The effects of electron-electron interactions are considered to be relatively small in double-barrier structures with low barriers. The motion of the electrons is governed by the double-barrier potential and the interface-roughness scattering. Since we are dealing with elastic tunneling the current density can be found from the standard "Landauer-type" formula,

$$j = 2e \int_{k_z>0} \frac{d^3k}{(2\pi)^3} \frac{\hbar k_z}{m^*} T(\mathbf{k}) \, [n_L(\varepsilon_\mathbf{k}) - n_R(\varepsilon_\mathbf{k})], \tag{2}$$

where e is the elementary charge and $\mathbf{k}$ is the wave vector (in the left contact) of the electron impinging from the left. We have used the GaAs value $m^* = 0.067m_0$ for the electron effective mass throughout the whole structure. When calculating the occupation numbers in the left and right contacts, n_L and n_R respectively, we assume that the chemical potential differs by eU between the contacts, U being the bias voltage. Moreover, we evaluate the occupation numbers at zero temperature; we are primarily going to compare with a low-temperature experiment. To calculate the transmission probability T we must solve for the electron wave function. To the right of the DBS it is a sum of outgoing waves,

$$\psi_\mathbf{k}(\mathbf{r}) = \sum_{\mathbf{k}'} t(\mathbf{k}', \mathbf{k}) \, e^{ik_z' z} \, e^{i\mathbf{k}_\parallel' \cdot \mathbf{r}_\parallel}. \tag{3}$$

The transmission probability is then

$$T(\mathbf{k}) = \sum_{\mathbf{k}'} \frac{k_z'}{k_z} \langle |t(\mathbf{k}', \mathbf{k})|^2 \rangle, \tag{4}$$

where $\mathbf{k}'$ is the final-state wave vector. The angular brackets indicate averaging over different interface-roughness configurations. We refer to the Appendix for the calculation of the reflection probability. The absolute magnitudes of the wave vectors are related to the total energy ε by

$$\varepsilon = \frac{\hbar^2 k^2}{2m^*} = \frac{\hbar^2 k'^2}{2m^*} - eU. \tag{5}$$

For a given interface-roughness configuration, described by the potential V_{IR}, the wave function satisfies the Lippmann-Schwinger equation (we omit the subscript $\mathbf{k}$)

$$\psi(\mathbf{r}) = \psi_0(\mathbf{r}) + \int d^3r' \, G_0(\mathbf{r}, \mathbf{r}') V_{\mathrm{IR}}(\mathbf{r}') \psi(\mathbf{r}'), \tag{6}$$

where the integration runs over all space. In this equation ψ_0 is the electron wave function in the absence of interface-roughness scattering satisfying

$$\left[-\frac{\hbar^2}{2m^*} \nabla^2 + V_{\mathrm{DBS}}(\mathbf{r}) - \varepsilon \right] \psi_0(\mathbf{r}) = 0 \tag{7}$$

and the Green's function G_0 is the solution of

$$\left[-\frac{\hbar^2}{2m^*} \nabla^2 + V_{\mathrm{DBS}}(\mathbf{r}) - \varepsilon \right] G_0(\mathbf{r}, \mathbf{r}', \varepsilon) = -\delta^{(3)}(\mathbf{r} - \mathbf{r}'), \tag{8}$$

satisfying the boundary condition of outgoing waves away from the interface roughness. The explicit appearance of the potential V_{IR} in Eq. (6) poses a problem when averaging over different interface-roughness configurations. The potential can, however, be eliminated by comparing Eq. (6) with its counterpart for the dressed Green's function G in the presence of interface roughness:

$$G(\mathbf{r}, \mathbf{r}', \varepsilon) = G_0(\mathbf{r}, \mathbf{r}', \varepsilon) + \int d^3r'' \, G_0(\mathbf{r}, \mathbf{r}'', \varepsilon) V_{IR}(\mathbf{r}'') G(\mathbf{r}'', \mathbf{r}', \varepsilon). \tag{9}$$

From Eq. (9) we get the formal identity $[1 - G_0 V_{\mathrm{IR}}]^{-1} = G G_0^{-1}$, so the Lippmann-Schwinger equation can now be written

$$\psi(\mathbf{r}) = \int d^3r' \int d^3r'' \, G(\mathbf{r}, \mathbf{r}', \varepsilon) G_0^{-1}(\mathbf{r}', \mathbf{r}'', \varepsilon) \psi_0(\mathbf{r}''). \tag{10}$$

In this formula all effects of the interface roughness are contained in $G(\mathbf{r}, \mathbf{r}')$. The introduction of the inverse Green's function G_0^{-1} is thus convenient from a formal point of view. We should point out that G_0^{-1} does not appear in the final expressions for the transmission probability, etc. Since the unperturbed system is translationally invariant parallel to the barriers we Fourier transform the Green's functions in the x and y variables:

$$G(\mathbf{r}, \mathbf{r}', \varepsilon) = \int \frac{d^2k_\parallel}{(2\pi)^2} \int \frac{d^2k_\parallel'}{(2\pi)^2} \, e^{i\mathbf{k}_\parallel \cdot \mathbf{r}_\parallel} G(\mathbf{k}_\parallel, \mathbf{k}_\parallel', z, z', \varepsilon) \times e^{-i\mathbf{k}_\parallel' \cdot \mathbf{r}_\parallel'}, \tag{11a}$$

$$G_0^{-1}(\mathbf{r}, \mathbf{r}', \varepsilon) = \int \frac{d^2k_\parallel}{(2\pi)^2} \, e^{i\mathbf{k}_\parallel \cdot (\mathbf{r}_\parallel - \mathbf{r}_\parallel')} G_0^{-1}(\mathbf{k}_\parallel, z, z', \varepsilon). \tag{11b}$$

The unperturbed wave function is

$$\psi_0(\mathbf{r}) = e^{i\mathbf{k}_\parallel \cdot \mathbf{r}_\parallel} \phi_{0\kappa}(z), \tag{12}$$

where $\phi_{0\kappa}(z)$ is the solution of the one-dimensional

Schrödinger equation

$$\left[-\frac{\hbar^2}{2m^*}\frac{d^2}{dz^2}+V_{\rm DBS}(z)-\varepsilon_z\right]\phi_{0\kappa}(z)=0, \tag{13}$$

with an incoming plane wave from the left and outgoing reflected and transmitted waves to the left and right, respectively. The energy associated with the motion in the z direction $\varepsilon_z=\varepsilon-\hbar^2\kappa^2/2m^*$ and the symbol κ denotes the absolute magnitude of $\mathbf{k}_\parallel$. For $\mathbf{r}$ to the right of the double-barrier structure the wave function of an electron with initial momentum $\mathbf{k}$ can be written as

$$\psi(\mathbf{r})=\int_{-\infty}^{\infty}dz'\int_{-\infty}^{\infty}dz''\int\frac{d^2k'_\parallel}{(2\pi)^2}\,G(\mathbf{k}'_\parallel,\mathbf{k}_\parallel,z,z',\varepsilon)\times G_0^{-1}(\mathbf{k}_\parallel,z',z'',\varepsilon)\phi_{0\kappa}(z''). \tag{14}$$

The dressed Green's function G is the only quantity that depends on the interface roughness in this expresssion. The configuration-averaged value of $|t|^2$ is found by evaluating the absolute square of $\psi(\mathbf{r})$ at any point with a z-coordinate z_R to the right of the DBS:

$$\langle|t(\mathbf{k}',\mathbf{k})|^2\rangle=\int_{-\infty}^{\infty}dz_1\int_{-\infty}^{\infty}dz_2\int_{-\infty}^{\infty}dz_3\int_{-\infty}^{\infty}dz_4\langle G^*(\mathbf{k}'_\parallel,\mathbf{k}_\parallel,z_R,z_1,\varepsilon)G(\mathbf{k}'_\parallel,\mathbf{k}_\parallel,z_R,z_3,\varepsilon)\rangle\times G_0^{-1*}(\mathbf{k}_\parallel,z_1,z_2,\varepsilon)G_0^{-1}(\mathbf{k}_\parallel,z_3,z_4,\varepsilon)\phi^*_{0\kappa}(z_2)\phi_{0\kappa}(z_4). \tag{15}$$

Except for the roughness-averaged product $\langle G^*G\rangle$ of the dressed Green's functions all quantities in Eq. (15) can be calculated once the double-barrier potential is known.

There are two different contributions, illustrated in Figs. 2(a) and 2(b), to the right-hand side of Eq. (15). The first of these contributions come from unscattered electrons, the second from electrons that have been scattered by the interface roughness. We now make two general assumptions about the scattering potential: (i) it is localized to a single plane $z=z_0$, and (ii) it is cylindrically symmetric (i.e., the strength of the scattering potential does not depend on the absolute orientations of the initial and final momenta of an electron). We then find

$$\langle|t(\mathbf{k}',\mathbf{k})|^2\rangle=\int_{-\infty}^{\infty}dz_1\int_{-\infty}^{\infty}dz_2\int_{-\infty}^{\infty}dz_3\int_{-\infty}^{\infty}dz_4\,[\,\delta_{\mathbf{k}'_\parallel,\mathbf{k}_\parallel}\,G^*_\kappa(z_R,z_1,\varepsilon)G^{-1*}_{0\kappa}(z_1,z_2,\varepsilon)\phi^*_{0\kappa}(z_2)G_\kappa(z_R,z_3,\varepsilon)\times G^{-1}_{0\kappa}(z_3,z_4,\varepsilon)\phi_{0\kappa}(z_4)$$
$$+\,G^*_{\kappa'}(z_R,z_0,\varepsilon)G^*_\kappa(z_0,z_1,\varepsilon)G^{-1*}_{0\kappa}(z_1,z_2,\varepsilon)\phi^*_{0\kappa}(z_2)\times\Lambda(\mathbf{k}',\mathbf{k},\varepsilon)G_{\kappa'}(z_R,z_0,\varepsilon)G_\kappa(z_0,z_3,\varepsilon)G^{-1}_{0\kappa}(z_3,z_4,\varepsilon)\phi_{0\kappa}(z_4)\,]. \tag{16}$$

In this equation we have used the notation $G_\kappa=G(\mathbf{k}_\parallel,\mathbf{k}_\parallel)$, etc., since all the Green's functions describe the propagation of an electron from a particular momentum, back to the very same momentum, and moreover these Green's functions only depend on the magnitude of the parallel momentum when the scattering potential is cylindrically symmetric. The vertex function $\Lambda(\mathbf{k}',\mathbf{k},\varepsilon)$ describes the rate at which real scattering events from $\mathbf{k}$ to $\mathbf{k}'$ take place.[29] To lowest order Λ is proportional to the absolute square of the interface-roughness scattering matrix element. The higher-order contributions to Λ take into account multiple-scattering events. The detailed calculation of Λ will be discussed in the next subsection [see Eq. (26)].

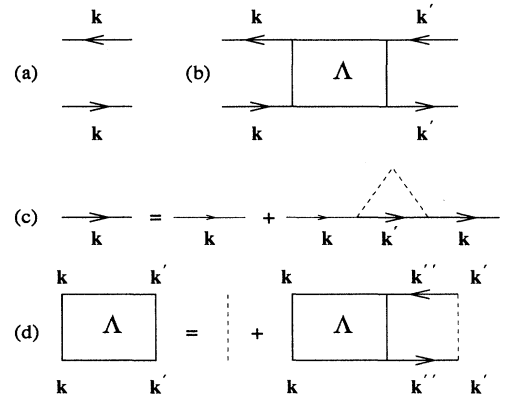

FIG. 2. Diagrammatic illustration of the calculations. (a) Contribution to the transmission probability from unscattered electrons and (b) from electrons that have been scattered by the interface roughness. (c) The Dyson equation relating the dressed Green's function to the bare one. The self-energy insertion is calculated within the self-consistent Born approximation. (d) Illustration of the integral equation for the vertex function Λ.

To carry out the integrations over the z variables in Eq. (16) we must relate the roughness-averaged dressed Green's functions G, to the bare ones G_0, through the Dyson equation. When all interface-roughness scattering takes place in the plane $z=z_0$ the self-energy Σ takes the form

$$\Sigma_{\mathbf{k}_\parallel}(z,z',\varepsilon)=\sigma_\kappa(\varepsilon)\delta(z-z_0)\delta(z'-z_0). \tag{17}$$

Thus we can write the Dyson equation, describing the propagation of an electron from momentum $\mathbf{k}$ back to the same momentum via two interface-roughness scattering events, as

$$G_\kappa(z,z',\varepsilon)=G_{0\kappa}(z,z',\varepsilon)+G_{0\kappa}(z_0,z',\varepsilon)\sigma_\kappa(\varepsilon)G_\kappa(z,z_0,\varepsilon). \tag{18}$$

This equation[30] is illustrated in Fig. 2(c) and it has the formal solution

$$G_\kappa(z,z',\varepsilon) = G_{0\kappa}(z,z',\varepsilon) + \frac{G_{0\kappa}(z_0,z',\varepsilon)\sigma_\kappa(\varepsilon)G_{0\kappa}(z,z_0,\varepsilon)}{1-\sigma_\kappa(\varepsilon)G_{0\kappa}(z_0,z_0,\varepsilon)}. \quad (19)$$

The bare Green's function is easily calculated from

$$G_{0\kappa}(z,z',\varepsilon) = \frac{\phi_{L\kappa}(z_<)\phi_{R\kappa}(z_>)}{W}. \quad (20)$$

The wave functions $\phi_{L\kappa}$ and $\phi_{R\kappa}$ satisfy Eq. (13) and give outgoing waves to the left (L) and right (R) of the DBS, respectively. The model potential we use is constant in the contacts and piecewise linear across the barriers and the quantum well. Thus both $\phi_{L\kappa}$ and $\phi_{R\kappa}$ can be expressed in terms of Airy functions in the barriers and the quantum well and in terms of plane waves in the contacts. The coordinate $z_<$ ($z_>$) is the lesser (greater) of z and z', and W denotes the Wronskian,

$$W = \phi_{L\kappa}\phi'_{R\kappa} - \phi'_{L\kappa}\phi_{R\kappa}. \quad (21)$$

Inserting Eq. (19) into Eq. (16) and using

$$\int_{-\infty}^{\infty} dz'' G_{0\kappa}(z,z'',\varepsilon)G_{0\kappa}^{-1}(z'',z',\varepsilon) = \delta(z-z')$$

we find

$$\langle|t(\mathbf{k}',\mathbf{k})|^2\rangle = \delta_{\mathbf{k}'_\parallel,\mathbf{k}_\parallel}\left|\phi_{0\kappa}(z_R) + \frac{\sigma_\kappa(\varepsilon)G_{0\kappa}(z_R,z_0,\varepsilon)}{1-\sigma_\kappa(\varepsilon)G_{0\kappa}(z_0,z_0,\varepsilon)}\phi_{0\kappa}(z_0)\right|^2 + \left|\frac{G_{0\kappa'}(z_R,z_0,\varepsilon)}{1-\sigma_{\kappa'}(\varepsilon)G_{0\kappa'}(z_0,z_0,\varepsilon)}\right|^2 \Lambda(\mathbf{k}',\mathbf{k},\varepsilon)\left|\phi_{0\kappa}(z_0) + \frac{\sigma_\kappa(\varepsilon)G_{0\kappa}(z_0,z_0,\varepsilon)}{1-\sigma_\kappa(\varepsilon)G_{0\kappa}(z_0,z_0,\varepsilon)}\phi_{0\kappa}(z_0)\right|^2. \quad (22)$$

This result can now be inserted into Eq. (4) and subsequently Eq. (2) when calculating the tunnel current, but we still must determine $\sigma_\kappa(\varepsilon)$ and the vertex function $\Lambda(\mathbf{k}',\mathbf{k},\varepsilon)$. This will be done in the next subsection.

B. Calculation of the self-energy and the vertex function

In order to get results that preserve unitarity it is essential to employ the same kind of approximations in both the self-energy and vertex-function calculations.[29] Here we use the self-consistent Born approximation (SCBA). A diagrammatic illustration of the self-energy is given in Fig. 2(c). The vertex function is calculated in Fig. 2(d). The SCBA is a multiple-scattering formalism. An electron can undergo any number of scattering events while it is in the quantum well. However, the interaction with an interface-roughness island is treated to lowest order at each encounter. It is fairly straightforward to generalize the SCBA to take into account scattering to all orders at each encounter with a roughness island. This corresponds to the coherent-potential approximation (CPA).[31] Common to both the SCBA and the CPA is that they do not account explicitly for interference effects between different roughness islands. All Feynman diagrams with crossed interaction lines are neglected. So-called maximally crossed diagrams[32] are known to describe coherent backscattering. This effect has been studied in the context of an optical Fabry-Pérot cavity (resonant tunneling of photons) by Berkovits and Feng.[23] We think it is safe to neglect this effect in the present calculation. The maximally crossed diagrams give strong scattering from $\mathbf{k}_\parallel$ to $-\mathbf{k}_\parallel$, but this should not change the tunnel current substantially. Coherent backscattering can in any case not bring an off-resonant electron into resonance since it does not change the parallel-motion kinetic energy.

Turning to the detailed calculation we first have to decide what scattering potential to use. In the experiment the interface-roughness consists of islands of barrier material penetrating into the quantum well or vice versa. Typically these islands have a radius $\rho_0 \sim 100$ Å and their height h_i corresponds to one to two atomic layers.[3,4] The height is small compared with the width of the quantum well, so we can replace the island's extension perpendicular to the barriers with a delta function $h_i\delta(z-z_0)$, where z_0 is the location of the downstream inner wall of the quantum well. We choose to place the interface roughness at one single interface. The primary reason for this is that the interfaces of MBE-grown heterostructures are different depending on in which order the layers are grown. The interface one gets when growing $Al_xGa_{1-x}As$ on top of GaAs has considerably larger islands than in the opposite case and is therefore more efficient in assisting resonant tunneling. We place the roughness on the downstream wall because it has larger effect there when the DBS is biased. The difference between the two surfaces leads to an asymmetry in the current-voltage characteristics which has both been observed experimentally[5] and found in earlier theoretical calculations.[21] If we furthermore assume that the interface-roughness islands are circular in shape with a radius ρ_0, consistent with the typical island area $A_i = \pi\rho_0^2$, the Fourier transform of the potential in two dimensions is (for an island centered at the origin)

$$V(\mathbf{k}_\parallel) = \int_0^{\rho_0}\rho\,d\rho\int_0^{2\pi} d\varphi V_b e^{-i\kappa\rho\cos\varphi} = 2A_iV_b\frac{J_1(\kappa\rho_0)}{\kappa\rho_0}. \quad (23)$$

Here V_b is the barrier height and J_1 is an ordinary Bessel function. In reality the different islands have different sizes and different shapes. It is therefore reasonable to keep only the central peak (around $\kappa = 0$) of the above

potential. We do this by approximating $V(\mathbf{k}_\parallel)$ by a Gaussian function

$$V(\mathbf{k}_\parallel) \approx A_i V_b e^{-\alpha\kappa^2}, \tag{24}$$

where $\alpha = 0.15\rho_0^2$ (see Fig. 3). As is seen from Eq. (24) the effects of the interface-roughness scattering vanishes both when $A_i \to 0$ and when $A_i \to \infty$. Islands with a radius $\rho_0 \approx 75$ Å are the most efficient in increasing the valley current by assisting resonant tunneling through the DBSs we are going to consider. We find this by optimizing $n_i|V(\mathbf{k}_\parallel)|^2$ while keeping the coverage $n_i A_i$ constant (recall that n_i is the areal density of interface-roughness islands) and assuming that the momentum transfer corresponds to 30 meV ($= \hbar^2\kappa^2/2m^*$).

We can now calculate $\sigma_\kappa(\varepsilon)$ and $\Lambda(\mathbf{k}', \mathbf{k}, \varepsilon)$. The Fourier transform of the scattering potential from a roughness island away from the origin carries a phase factor. Thus, when roughness averaging only products $V(\mathbf{k}_\parallel)V(-\mathbf{k}_\parallel) = |V(\mathbf{k}_\parallel)|^2$ give nonzero results. From the insertion in Fig. 2(c) we get the following expression for the self-energy:

$$\sigma_\kappa(\varepsilon) = n_i h_i^2 \int \frac{d^2k_\parallel'}{(2\pi)^2} |V(\kappa\hat{x} - \mathbf{k}_\parallel')|^2 G_{\kappa'}(z_0, z_0, \varepsilon). \tag{25}$$

We have taken the parallel momentum of the electron to point in the x direction; the self-energy does not depend on the direction of $\mathbf{k}$ because the scattering potential is cylindrically symmetric. Equation (25) has to be solved by iteration since the Green's function appearing in the integral itself depends on $\sigma_{\kappa'}(\varepsilon)$.

The integral (Bethe-Salpeter) equation for $\Lambda(\mathbf{k}', \mathbf{k}, \varepsilon)$ illustrated in Fig. 2(d) becomes

$$\begin{aligned}\Lambda(\mathbf{k}', \mathbf{k}, \varepsilon) = {} & n_i h_i^2 |V(\mathbf{k}_\parallel' - \mathbf{k}_\parallel)|^2 \\ & + n_i h_i^2 \int \frac{d^2k_\parallel''}{(2\pi)^2} |G_{\kappa''}(z_0, z_0, \varepsilon)|^2 \\ & \times |V(\mathbf{k}_\parallel' - \mathbf{k}_\parallel'')|^2 \Lambda(\mathbf{k}'', \mathbf{k}, \varepsilon).\end{aligned} \tag{26}$$

Once again thanks to the cylindric symmetry of the scattering potential, Λ only depends on the absolute magnitudes of $\mathbf{k}_\parallel'$ and $\mathbf{k}_\parallel$ and their relative angle. In the calculation of the tunnel current we can thus let $\mathbf{k}_\parallel$ point in the x direction. Moreover, in order to calculate the transmission probability $T(\mathbf{k})$ it suffices to know the angle-averaged vertex function $\overline{\Lambda}(\kappa', \kappa, \varepsilon)$ defined by

$$\overline{\Lambda}(\kappa', \kappa, \varepsilon) = \frac{1}{2\pi} \int_0^{2\pi} d\varphi \Lambda\{\kappa'[\hat{x}\cos(\varphi) + \hat{y}\sin(\varphi)], \kappa\hat{x}, \varepsilon\}. \tag{27}$$

Applying the angular-averaging procedure to the Bethe-Salpeter equation with the potential in Eq. (24) yields

$$\begin{aligned}\overline{\Lambda}(\kappa', \kappa, \varepsilon) = {} & n_i h_i^2 A_i^2 V_b^2 e^{-2\alpha(\kappa'^2+\kappa^2)} I_0(4\alpha\kappa'\kappa) \\ & + n_i h_i^2 A_i^2 V_b^2 \int_0^{\kappa_{\max}} \frac{\kappa'' d\kappa''}{2\pi} e^{-2\alpha(\kappa'^2+\kappa''^2)} I_0(4\alpha\kappa'\kappa'') |G_{\kappa''}(z_0, z_0, \varepsilon)|^2 \overline{\Lambda}(\kappa'', \kappa, \varepsilon),\end{aligned} \tag{28}$$

where I_0 is a modified Bessel function of the first kind. We have introduced a truncation of the basis set at a maximum parallel kinetic energy $\varepsilon_{\max} = \hbar^2\kappa_{\max}^2/2m^*$. The states that are removed in this way have no practical importance for the tunneling; the only thing that is important to keep in mind is that the same truncation must be made when calculating the self-energy in Eq. (25). The truncation of the basis set simplifies the solution of the integral equation; it becomes termwise separable if we expand $\overline{\Lambda}$ and the potential from an interface-roughness island in double sums of Chebyshev polynomials:[33]

$$\begin{aligned}\overline{\Lambda}(\kappa', \kappa, \varepsilon) = {} & \sum_{j',j=1}^{M} \lambda_{j'j}(\varepsilon) \\ & \times T_{j'-1}\left(\hbar^2\kappa'^2/m^*\varepsilon_{\max} - 1\right) \\ & \times T_{j-1}\left(\hbar^2\kappa^2/m^*\varepsilon_{\max} - 1\right),\end{aligned} \tag{29a}$$

$$\begin{aligned}& e^{-2\alpha(\kappa'^2+\kappa^2)} I_0(4\alpha\kappa'\kappa) \\ & = \sum_{j',j=1}^{M} v_{j'j} T_{j'-1}\left(\hbar^2\kappa'^2/m^*\varepsilon_{\max} - 1\right) \\ & \quad \times T_{j-1}\left(\hbar^2\kappa^2/m^*\varepsilon_{\max} - 1\right).\end{aligned} \tag{29b}$$

In the actual numerical calculations we used $\varepsilon_{\max}$ =100 meV and M =15. The coefficients $v_{j'j}$ can be calculated once and for all for a given value of α. The explicit expression is

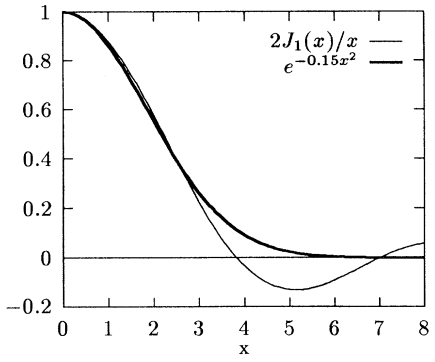

FIG. 3. Comparison between the functions describing the interface-roughness potential in Eqs. (23) and (24).

$$v_{j'j} = \frac{(2-\delta_{j',1})(2-\delta_{j,1})}{N^2} \times \sum_{l,l'=1}^{N} \exp\left[-2\alpha\frac{m^*\varepsilon_{\max}}{\hbar^2}(\zeta_{l'}+\zeta_l+2)\right] \times I_0\left[4\alpha\frac{m^*\varepsilon_{\max}}{\hbar^2}\sqrt{(\zeta_{l'}+1)(\zeta_l+1)}\right] \times T_{j'-1}(\zeta_{l'})T_{j-1}(\zeta_l), \quad (30)$$

where

$$\zeta_l = \cos\left(\frac{\pi(l-\frac{1}{2})}{N}\right). \quad (31)$$

We used $N=50$ in this calculation.

Solving the integral equation now reduces to determining the coefficients $\lambda_{j'j}(\varepsilon)$. If one inserts Eqs. (29a) and (29b) into Eq. (28) and calculates the matrix elements

$$P_{l'l}(\varepsilon) = \int_0^{\kappa_{\max}} \frac{\kappa'' d\kappa''}{2\pi} |G_{\kappa''}(z_0,z_0,\varepsilon)|^2 \times T_{l'-1}\left(\hbar^2\kappa''^2/m^*\varepsilon_{\max}-1\right) \times T_{l-1}\left(\hbar^2\kappa''^2/m^*\varepsilon_{\max}-1\right) \quad (32)$$

and the matrix product

$$Q_{j'l}(\varepsilon) = \sum_{l'=1}^{M} v_{j'l'}P_{l'l}(\varepsilon), \quad (33)$$

it is found that the coefficients $\lambda_{j'j}$ satisfy

$$\lambda_{j'j}(\varepsilon) = n_i h_i^2 A_i^2 V_b^2 v_{j'j} + n_i h_i^2 A_i^2 V_b^2 \sum_{l=1}^{M} Q_{j'l}(\varepsilon)\lambda_{lj}(\varepsilon). \quad (34)$$

A matrix inversion yields

$$\lambda_{j'j}(\varepsilon) = \sum_{l=1}^{M} [[1 - n_i h_i^2 A_i^2 V_b^2 Q]^{-1}]_{j'l} n_i h_i^2 A_i^2 V_b^2 v_{lj}. \quad (35)$$

Now we insert Eq. (22) into Eq. (4). Since Λ is the only quantity entering the expression for $\langle|t|^2\rangle$ that depends on the direction of $\mathbf{k}'$, the angular integration transforms $\Lambda(\mathbf{k}',\mathbf{k},\varepsilon)$ into $\overline{\Lambda}(\kappa',\kappa,\varepsilon)$. From then on the knowledge of the coefficients $\lambda_{j'j}(\varepsilon)$ makes it possible to calculate the transmission probability and the tunnel current.

III. RESULTS AND DISCUSSION

Figure 4(a) shows how the scattering changes the transmission probability of an electron as a function of its initial z-motion energy ε_z. The interface roughness islands have area $A_i = 4\times10^4$ Å^2 and their height is $h_i =$ 5 Å, which corresponds to almost two atomic layers. The areal density of islands n_i is 10^{-5} Å^{-2}, i.e., 40% of the interface is covered with islands with these parameter values. The barriers are $d=70$ Å thick and $V_b=120$ meV high in this calculation. The quantum well is $L=70$ Å wide. We use quite narrow barriers in order to be able to compare the transmission probabilities in the same figure. The transmission peak is fairly sharp when there is no scattering present. The peak value is less than 1 because the DBS is biased with $U=70$ mV and thus asymmetric, so perfect transmission cannot be obtained for any energy. The transmission resonance is suppressed and broadened when interface-roughness scattering is included in the calculation. When the initial parallel momentum of the electron equals zero we get an asymmetric transmission resonance. In this case the parallel-motion energy must increase in the scattering events that assist resonant tunneling. This is only possible if the electron's

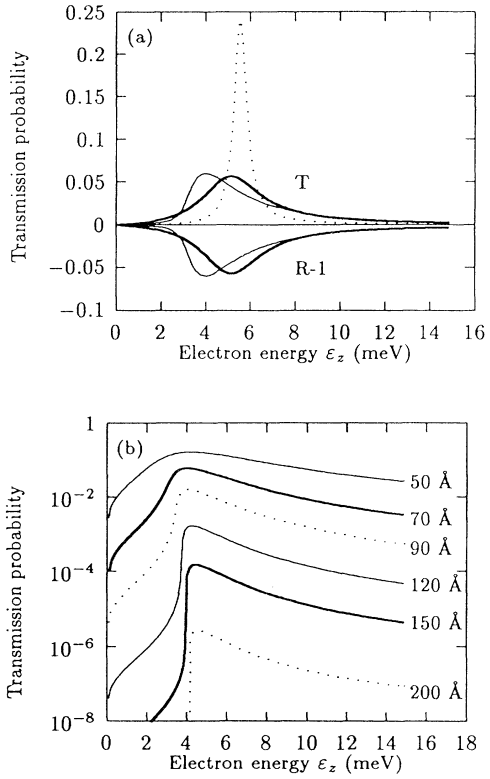

FIG. 4. The transmission probability of an electron as a function of its initial "z-motion energy." (a) The DBS has 70-Å-thick barriers and a 70-Å-wide quantum well. The barriers are 120 meV high and the bias voltage is 70 mV. The dotted curve gives the transmission probability with no interface roughness present. In the other calculations the downstream inner wall of the quantum well was covered by roughness islands. The areal density of islands was $n_i = 10^{-5}$ Å^{-2}, each island had area $A_i = 4\times10^4$ Å^2, and height $h_i = 5$ Å. The thin-line curves give T, and $R-1$, of electrons with initial "parallel" kinetic energy $\varepsilon_\parallel = 0$. The thick curves have been calculated with an initial $\varepsilon_\parallel = 3$ meV. (b) Transmission probability on a logarithmic scale for a DBS with the same interface-roughness parameter values as in (a). The DBS is also the same except for the barrier thickness which is varied as indicated to the right of the curves. The initial $\varepsilon_\parallel$ is zero.

ε_z is larger than the resonant level energy. One therefore gets a sharp edge on the low-energy side and a long tail on the high-energy side of the resonance. We also see that the peak position is shifted towards lower energy. The real part of the self energy is negative since the $\mathbf{k}_{||} = \mathbf{0}$ state is only coupled to states of higher energy by the interface roughness. With a finite initial parallel momentum the transmission resonance is more symmetric and less shifted towards lower energy.

In Fig. 4(a) we also display two plots of $R - 1$, where R is the reflection probability. We see that these curves are the mirror images of the corresponding curves for the transmission probability. This shows that the calculation gives results that preserve unitarity ($R + T = 1$). Numerically $R + T$ differs from 1 by less than 10^{-7} in our calculations.

If the barrier thickness is increased it becomes, in an average sense, more difficult for an electron to tunnel through. This changes the no-scattering and scattering transmission probabilities in different ways. The width of the sharp peak in the no-scattering case decreases with increasing barrier thickness. This is due to the fact that the electron's intrinsic lifetime in the quantum well increases. The transmission probability with interface-roughness scattering present, on the other hand, gets more and more suppressed while its width, which is primarily determined by the scattering lifetime, does not change too much. This is shown in Fig. 4(b).

In Fig. 5 we compare the tunnel current through a DBS with thick barriers with and without interface-roughness scattering. In this calulation the barrier thickness was $d = 250$ Å, the well width was $L = 70$ Å, and the Fermi energy of the electron gas in the doped emitter contact was taken to be $E_F = 15$ meV. The parameter values for the interface roughness are the same as those used in Fig. 4. On the linear scale in Fig. 5(a) we see that the peak current is reduced by about 10% when allowing for scattering. The peak is at the same time somewhat broadened. We can explain this behavior by taking a look at Fig. 4: A tunneling electron is scattered many times while inside the quantum well. The net effect of this is that the spectral strength associated with the resonant level in the quantum well is redistributed from a very sharp peak to a broad but suppressed resonance. The tunnel current is, however, an integrated quantity and it does not change much even if the underlying transmission probability changes as long as the broadening of the resonance is not larger than the width of the energy distribution of the incoming electrons. These results are in general agreement with the conclusions drawn from early phenomenological models.[34–36]

In Fig. 5(b) the tunnel current is plotted on a logarithmic scale. Here we see that the valley current increases by several orders of magnitude when interface-roughness scattering is included in the calculations. The current density has been calculated using two different values for the areal density of roughness islands. The higher value of n_i was basically chosen in order to account for other scattering mechanisms (roughness at other interfaces, alloy scattering, etc.) in an approximate way. We see that increasing the number of scatterers by a factor of 2 gives a corresponding reduction of the P/V ratio. It is worth noticing that both the general shape of the current-voltage characteristics and the P/V ratio in this latter case begins to resemble the experimental results.[6]

We have also performed a calculation in which the interface roughness is treated to lowest order in perturbation theory. This is the approximation used by Leo and MacDonald.[22] The at first surprising result is that the perturbative and nonperturbative calculations give values of the valley current that are practically identical (the difference is less than 1%). In the perturbative calculation electrons are scattered into a very sharp resonance, while in the nonperturbative case they are scattered into a broadened resonance. The integrated spectral strength of the resonance is, however, basically the same in both cases. Moreover, the very first scattering event is the all important one. It must bring the electron close to resonance. This can be understood from the following reasoning: With the parameter values given in Fig. 5, an electron entering the quantum well at a 130-mV bias is off resonance by ≈30 meV. Thus the uncertainty relation allows the electron to stay in the quantum well (in a virtual state) for ∼0.02 ps. This is considerably shorter than the scattering lifetime and one cannot expect more

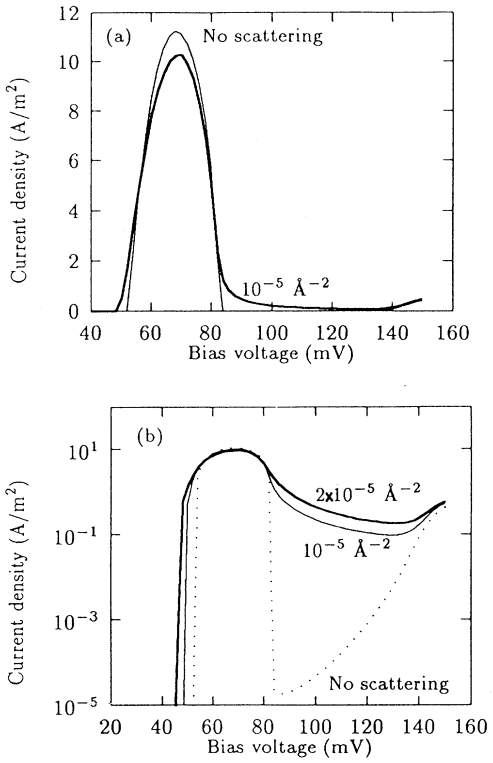

FIG. 5. The current-voltage characteristics of a double-barrier structure with d =250 Å, L =70 Å, and V_b =120 meV, at zero temperture on (a) a linear scale and (b) a logarithmic scale. The Fermi energy of the electron gases in the doped contacts is 15 meV. The parameter values for the interface roughness are the same as in Fig. 4, except for the areal density n_i of roughness islands which is given next to the curves.

than one scattering event to take place in that time span. This explains why the perturbative and nonperturbative calculations give nearly equal results for the valley current.

To get considerable differences between the results of the two calculations one must use unrealistically large parameter values for the interface roughness, so that the width of the transmission resonance in the SCBA calculation becomes comparable to the difference between the valley and peak voltages. When this happens the perturbative calculation gives too large values for the valley current compared with the correct value.

It is particularly interesting to compare the calculated peak-to-valley ratios with the ones that are found from experiment. In Fig. 6 we have plotted our calculated P/V ratios as a function of barrier thickness. The parameter values describing the DBS are taken from the experiment by Guéret *et al.*[6] We see that the P/V ratio increases exponentially to begin with, but at $d \approx 100$ Å it starts to level off and then reaches a maximum at $d \approx 180$ Å. For even thicker barriers the P/V ratio decreases somewhat.

The exponential increase goes on as long as the intrinsic lifetime of an electron in the quantum well is shorter or comparable to the scattering lifetime. When this does not hold true any longer the P/V ratio levels off. Taking a look at Fig. 4(b) we see that the transmission probability through the three DBS's with the thickest barriers only differ by a constant factor (on the high-energy side of the peak). Thus the same crossover is seen also in this figure at $d \approx 100$ Å, and the underlying reason is that the intrinsic width of the transmission resonance becomes negligible in comparison with the scattering-induced broadening.

The decrease of the P/V ratio for barriers thicker than $d \approx 200$ Å is caused by the different looks of the barriers at the two different voltages. With "valley voltage" the barriers are more tilted and therefore a bit more transparent than in the "peak voltage" situation. This causes the decrease in P/V ratio. This effect is thus not directly connected to the interface-roughness scattering.

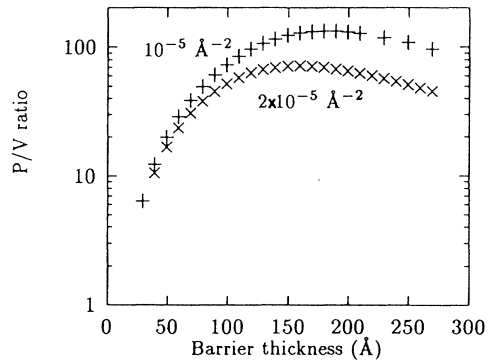

FIG. 6. The peak-to-valley ratio of the tunnel current through a DBS as a function of the barrier thickness. The areal density of scatterers is given in the figure, the rest of the DBS and interface-roughness parameters are the same as in Fig. 5.

Guéret *et al.* found the same qualitative behavior of the P/V ratio as a function of barrier thickness in their experiment.[6] Quantitatively their measured maximum P/V ratio was ≈ 20. We see that with $n_i = 2\times10^{-5}$ Å^{-2} the theoretical P/V ratio is a factor 3–4 larger than the experimental value. The DBS has in total four different interfaces. The perturbative calculation by Leo and MacDonald[22] showed that also the outer interfaces of the DBS give considerable contributions to the *valley* current. This result, in combination with our finding that perturbative and nonperturbative calculations give basically the same valley current, may indicate that it is justified to use even higher values for n_i than 2×10^{-5} Å^{-2}.

In any case our calculation shows that interface-roughness scattering can explain the qualitative behavior of the P/V ratio as a function of barrier thickness in a low-temperature experiment.[6] As for the magnitude of the maximum P/V ratio we find that it can be reduced to ≈ 50 with realistic parameter values for the interface roughness.

IV. SUMMARY

In this paper we have presented a calculation of the effects of interface-roughness scattering on resonant tunneling. We have treated the interface-roughness scattering to infinite order by means of the self-consistent Born approximation. The results show that the scattering does not change the peak current through the structure very much. The valley current, on the other hand, can, in the case of a DBS with thick barriers, increase by several orders of magnitude. When studying the calculated peak-to-valley ratio we find that it grows exponentially with increasing barrier thickness up to 100-Å-thick barriers. After that the increse is slower, and eventually a maximum is reached at a barrier thickness of about 200 Å. This is in good qualitative agreement with experiment. Finally, another important result of this work is that the valley current found from a calculation in which the interface-roughness scattering is treated by lowest-order perturbation theory is practically identical to the valley current found from a non-perturbative calculation.

ACKNOWLEDGMENTS

I thank Antti-Pekka Jauho for a number of very useful comments on the manuscript. The first part of this work was carried out while I was at the Facultés Universitaires Notre-Dame de la Paix in Namur, Belgium. I wish to thank Amand Lucas and his group for the hospitality. Financial support from the Belgian Program on Interuniversity Attraction Poles initiated by the Belgian State-Prime Minister's Office—Science Policy Programming is gratefully acknowledged.

APPENDIX

In this appendix we give the expressions for the reflection probability of an electron. To the left of the DBS

the electron wave function can be written as

$$\psi_{\mathbf{k}}(\mathbf{r}) = e^{ik_z z} e^{i\mathbf{k}_\parallel \cdot \mathbf{r}_\parallel} + \sum_{\mathbf{k}'} r(\mathbf{k}', \mathbf{k})\, e^{-ik_z' z}\, e^{i\mathbf{k}_\parallel' \cdot \mathbf{r}_\parallel}. \quad \text{(A1)}$$

This means that the reflection probability in analogy with Eq. (4) can be written as

$$R(\mathbf{k}) = \sum_{\mathbf{k}'} \frac{k_z'}{k_z} \langle |r(\mathbf{k}', \mathbf{k})|^2 \rangle. \quad \text{(A2)}$$

Note that both $\mathbf{k}$ and $\mathbf{k}'$ refer to the left-hand side of the DBS in this case. We thus have $|\mathbf{k}| = |\mathbf{k}'|$. The quantity $\langle |r(\mathbf{k}', \mathbf{k})|^2 \rangle$ is given by an expression analogous to Eq. (22),

$$\langle |r(\mathbf{k}', \mathbf{k})|^2 \rangle = \delta_{\mathbf{k}_\parallel', \mathbf{k}_\parallel} \left| \phi_{0\kappa}(0) + \frac{\sigma_\kappa(\varepsilon) G_{0\kappa}(0, z_0, \varepsilon)}{1 - \sigma_\kappa(\varepsilon) G_{0\kappa}(z_0, z_0, \varepsilon)} \phi_{0\kappa}(z_0) - 1 \right|^2$$
$$+ \left| \frac{G_{0\kappa'}(0, z_0, \varepsilon)}{1 - \sigma_{\kappa'}(\varepsilon) G_{0\kappa'}(z_0, z_0, \varepsilon)} \right|^2 \Lambda(\mathbf{k}', \mathbf{k}, \varepsilon) \left| \phi_{0\kappa}(z_0) + \frac{\sigma_\kappa(\varepsilon) G_{0\kappa}(z_0, z_0, \varepsilon)}{1 - \sigma_\kappa(\varepsilon) G_{0\kappa}(z_0, z_0, \varepsilon)} \phi_{0\kappa}(z_0) \right|^2, \quad \text{(A3)}$$

i.e., the reflected wave function has been evaluated at $z = 0$. The self-energy and vertex function should be calculated in the same way as when calculating the transmission probability.

[1] B. Ricco and M. Ya. Azbel, Phys. Rev. B **29**, 1970 (1984).
[2] V. J. Goldman, D. C. Tsui, and J. E. Cunningham, Phys. Rev. B **36**, 7635 (1987).
[3] B. A. Joyce, P. J. Dobson, J. H. Neave, and J. Zhang, Surf. Sci. **174**, 1 (1986).
[4] H. Sakaki, T. Noda, K. Hirakawa, M. Tanaka, and T. Matsusue, Appl. Phys. Lett. **51**, 1934 (1987).
[5] P. Guéret, C. Rossel, E. Marclay, and H. Meier, J. Appl. Phys. **66**, 278 (1989).
[6] P. Guéret, C. Rossel, W. Schlup, and H. P. Meier, J. Appl. Phys. **66**, 4312 (1989).
[7] L. I. Glazman and R. I. Shekhter, Solid State Commun. **66**, 65 (1988).
[8] N. S. Wingreen, K. W. Jacobsen, and J. W. Wilkins, Phys. Rev. Lett. **61**, 1396 (1988).
[9] M. Jonson, Phys. Rev. B **39**, 5924 (1989).
[10] A. P. Jauho, Phys. Rev. B **41**, 12 327 (1990).
[11] E. V. Anda and F. Flores, J. Phys. Condens. Matter **3**, 9087 (1991).
[12] J. A. Støvneng, E. H. Hauge, P. Lipavský, and V. Špička, Phys. Rev. B **44**, 13 595 (1991).
[13] R. Lake and S. Datta, Phys. Rev. B **45**, 6670 (1992).
[14] N. Zou and K. A. Chao, Phys. Rev. Lett. **69**, 3224 (1992).
[15] H. C. Liu and D. D. Coon, J. Appl. Phys. **64**, 6785 (1988).
[16] F. Chevoir and B. Vinter, Appl. Phys. Lett. **55**, 1859 (1989).
[17] F. Chevoir and B. Vinter, Phys. Rev. B **47**, 7260 (1993).
[18] H. A. Fertig and S. Das Sarma, Phys. Rev. B **40**, 7410 (1989).
[19] H. A. Fertig, S. He, and S. Das Sarma, Phys. Rev. B **41**, 3596 (1990).
[20] B. G. R. Rudberg, Semicond. Sci. Technol. **5**, 600 (1990).
[21] J. Leo and A. H. MacDonald, Phys. Rev. Lett. **64**, 817 (1990).
[22] J. Leo and A. H. MacDonald, Phys. Rev. B **43**, 9763 (1991).
[23] R. Berkovits and S. Feng, Phys. Rev. B **45**, 97 (1992).
[24] P. A. Schulz, Phys. Rev. B **43**, 4548 (1991).
[25] E. Runge and H. Ehrenreich, Phys. Rev. B **45**, 9145 (1992); Ann. Phys. (N.Y.) **219**, 55 (1992).
[26] M. Büttiker, Phys. Rev. B **33**, 3020 (1986); IBM J. Res. Dev. **32**, 63 (1988).
[27] S. Hershfield, Phys. Rev. B **43**, 11 586 (1991).
[28] P. Johansson, Phys. Rev. B **46**, 12 865 (1992).
[29] G. D. Mahan, *Many-Particle Physics* (Plenum, New York, 1990), pp. 601–634.
[30] Even though the superficial structure of this equation resembles that of Eq. (9), we wish to point out that they deal with somewhat different quantities. The Green's function in Eq. (9) corresponds to one specific roughness realization, while the Green's function in Eq. (18) is what results after roughness averaging.
[31] G. Rickayzen, *Green's Functions and Condensed Matter* (Academic, London, 1980), pp. 285–311.
[32] J. S. Langer and T. Neal, Phys. Rev. Lett. **16**, 984 (1966).
[33] W. H. Press, B. P. Flannery, S. A. Teukolsky, and W. T. Vetterling, *Numerical Recipes* (Cambridge University Press, Cambridge, 1989), pp. 147–151.
[34] A. D. Stone and P. A. Lee, Phys. Rev. Lett. **54**, 1196 (1985).
[35] T. Weil and B. Vinter, Appl. Phys. Lett. **50**, 1281 (1987).
[36] M. Jonson and A. Grincwajg, Appl. Phys. Lett. **51**, 1729 (1987).